



Stability Analysis of a Motor-Gear-Alternator (MGA) System Using Bode Plot Technique

Wesley Koech^{1*}

¹Department of Mathematics and Physics, School of Biological and Physical Sciences, Moi University, P.O.Box 3900-30100, Eldoret, Kenya.

Author's contribution

The sole author designed, analyzed and interpreted and prepared the manuscript.

Article Information

DOI: 10.9734/JAMCS/2017/37241

Editor(s):

(1) Junjie Chen, Professor, Department of Electrical Engineering, University of Texas at Arlington, USA.

Reviewers:

(1) Imdat Taymaz, Sakarya University, Turkey.

(2) Prashant Kumar, Savitribai Phule Pune University, India.

Complete Peer review History: <http://www.sciedomains.org/review-history/21746>

Received: 6th October 2017

Accepted: 31st October 2017

Published: 4th November 2017

Original Research Article

Abstract

Koech and the associates designed a Motor-Gear-Alternator (MGA) model and identified the effective parameters of that model. Nonetheless, the stability of the model to determine its applicability is still missing. In this paper, the author attempted to design a stable Motor-Gear Alternator (MGA) system using Bode plots criterion. The goal was to develop a system that could perform its design and intended functions without any interruptions. Simulation showed that the system is stable for $1 \leq \text{Gear ratio} \leq 7$ and the excess voltage is achieved when the Gear ratio > 3 . Moreover, when the Gear ratio is three, the system is stable with good response. This research has contributed to the field of system modeling, system identification and system stability analysis.

Keywords: Bode plots; motor; alternator and stability.

1 Objective

In this paper, the Bodes plots criterion is proposed as a technique for determining the stability of a Motor-Gear Alternator (MGA) system. The MGA system attempts to determine an optimum gear ratio for the realization of an optimum energy output.

*Corresponding author: E-mail: koech80@gmail.com;

2 Introduction

The stability of a system is a fundamental property contributing to system functionality and reliability [1]. Stability is a core factor that interest control engineers; especially during the design and analysis phases [2]. The optimum goal is to develop a system that is stable throughout its projected lifetime. Feedback control is an important tool for systems control. Feedback control reduces process variation and reduces the impact of disturbances. The design and analysis of system stability have a long history. As of 1905, the design and analysis processes were characterized by linearization and the analysis of roots of a given characteristic equation [3]. The stability of a power system is a vital issue in the planning and operation of a power system. The power system stabilizers utilize auxiliary stabilizing signals so as to regulate the excitation systems. The main focus of systems control is to achieve the improved power system dynamic performance [4].

The Bode plot is normally used to demonstrate the behavior of a transfer function. The Bode plot implies the analysis of the magnitude and the phase angle with respect to frequency. In general terms, an input signal expressed as $p_i(t) = \sin(\omega t)$ in a linear system will produce an output signal $q_o(t) = A \sin(\omega t + \varphi)$. The phase angle φ and the magnitude A dependent on the frequency [5]. Bode plots are adequate for examining the frequency behaviors of a given system; for instance, bandwidth identification. However, it remains a challenge, to use Bode plots for making zero analysis and precise poles as well as for characterizing complex frequencies. In addition, Bode plots are considered inadequate for evaluating the stability of a system with specific input signals; such as, input signals characterized by increasing ac signals and input signals that are exponentially decaying. The increasing ac signals are often observed [5]. Fortunately, in this paper the input signals of the MGA system are expected to be relatively steady constant thus Bode plot analysis will be adequate for analyzing its stability.

The circuit behavior can be observed only under the $j\omega$ axis while the zeros and the poles are well distributed on the whole s-plane, which is often a distance from the $j\omega$ axis. This complexity makes the detection of the zeros and the poles problematic and to be more likely inaccurate. A good example of a situation that the analysis difficult is when the zeros and poles which are close to each other but are distant from the $j\omega$ axis on the s-plane. Consequently, detection of the position of the zero and the pole becomes difficult with the utilization of conventional Bode plot approach [5]. Ideally, the roots, which comprises of the zeros and poles should be located on the $j\omega$ axis so that the peak can be observed in the Bode plot as the full signal passes through the root, thus, making signal detection easy [5].

The extraction of the zeros and poles of a transfer function is traditionally a two-step process. The initial step involves the creation of the denominator and the numerator polynomials; whereas, the second step is characterized by solving of the polynomials for the roots. It is observed that the symbolic extraction of the zeros and the poles have gained a significant ground over the years [6].

Several tools are available for solving polynomials for their roots via a numerical method. Key tools include MATHCAD, MATLAB, and other mathematical packages [5]. In this case, MATLAB is applied for solving the roots of the polynomials [6]. Most of the power system simulations are performed by use of the MATLAB software [4]. MATLAB is a simple since it is easy for one to input matrices and carryout calculations. Since its invention in 1981, the MATLAB Software has gained significant ground and use by the systems control community. The tool allows for simulation of finite state machines [3].

Bode plots were introduced by Nyquist and Bode back in the 1930S. Since then, the Bode diagrams have been employed in engineering and different fields of science. The real-time Bode diagrams of the MGA is possible with the MATLAB and other software such as LabVIEW (Laboratory Virtual Instrument Engineering Workbench) [7]. The sensitivity of a system to changes in various parameters is possible by plotting Bode plots [8]. Sensitivity analysis is performed to test the stability of the MGA system amid parameter changes.

Once an appropriate mathematical model of a system has been obtained, in transfer function form, the model is then analyzed to predict how the system will respond in both the time and frequency domains by using available mathematical tools. Transient Characteristics of Second Order Systems that store energy cannot respond instantaneously, so they exhibit a transient response when they are subjected to perturbed inputs or disturbances. Consequently, the transient response characteristics constitute one of the most important factors in system design [9]. Bode plot is a very useful technique for analyzing the stability of the closed-loop system [10]. The complex equation $G(j\omega)H(j\omega)$ might be shown by two separate graphs, one giving the magnitude against frequency and the phase angle (in degrees) versus the frequency. The logarithm of the magnitude $G(j\omega)H(j\omega)$ was used in the Bode diagram and the frequency is also plotted in the logarithmic scale, both for the amplitude and the phase angle [11].

The universal representation of the logarithmic magnitude of the $G(j\omega)H(j\omega)$ function is $20 \log_{10} |G(j\omega)H(j\omega)|$, whereby the base of the logarithm is 10 [12]. The unit utilized in the representation of the magnitude is the decibel, denoted as dB. In the logarithmic representation, the curves are structured on the semi-log paper, using the log scale for the frequency and the linear-scale for either magnitude (in dB) or the phase angle (in degrees). A number of techniques for analyzing the closed-loop transfer function have been proposed [13-15]. Specifically, several techniques which have used include [16] which studied Stability analysis of networked control systems, [13] analyzed the stability Closed-loop microwave amplifiers and [17] studied stability analysis for prioritized closed-loop inverse kinematic algorithms for redundant robotic systems.

The critical advantage of using the logarithmic plot for the frequency reaction of the transfer function is that multiplication of magnitudes resulted by individual factors can be estimated into addition [18]. Besides, it permits a simpler method for achieving the approximate log-magnitude curve of the transfer equation. It is based on straight-line asymptotic estimations, which is adequate for the rough sketching of the frequency response properties required in the design stage. When exact curves are required, corrections may be incorporated to these basic asymptotic plots. The utilization of logarithmic scale enables the display both in the low-frequency and high-frequency of the transfer function in a single graph. Even though the zero frequency cannot be involved in the logarithmic scale (since $\log 0 = \infty$), it is not a critical problem as one can assume a low a frequency since it is required for the analysis and the design of practical control system.

3 The Motor-Gear-Alternator Coupling

Fig. 1 is the system under study [19] whose transfer function is given by equation 1.

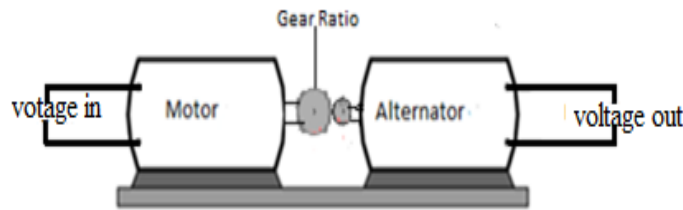


Fig. 1. Voltage relationship [19]

$$G(s) = \frac{V_a}{V_m} = G_r \left[\frac{-1186.73 S^2 - 4002.49 S - 3129.9}{13.54 S^2 + 59.20 S + 2.47} \right] \quad (1)$$

Equation (1) is the transfer function of MGA model [20] in which the stability is to be analyzed using the Bode plot criterion.

4 Closed Loop of MGA System

The principal factors that may be present in a transfer function $F(j\omega) = G(j\omega)H(j\omega)$, in general, are:

- i) Constant gain K
- ii) Pure integral and derivative factors $(j\omega)^{\pm n}$
- iii) First-order factors $(1 + j\omega T)^{\pm 1}$
- iv) Quadratic factors $[1 + 2\delta(j\omega/\omega_n) + (j\omega/\omega_n)^2]^{\pm 1}$

Following the identification of the basic factors of the logarithmic plots, it would be easy to add their contributions in a graphical representation to obtain the composite plot associated with the multiplying factors of $G(j\omega)H(j\omega)$, given that the product of terms adds up to their logarithms [21]. It will be observed that in the logarithmic scale, the real phase plots and amplitude of the key factors of $G(j\omega)H(j\omega)$ might be approximated via the utilization of straight line asymptotes that is an added advantage of the Bode plot. The errors of approximation are often definite and known. Corrections can be integrated easily to obtain an accurate plot.

4.1 Real constant gain K

$$\begin{aligned} F(j\omega) &= k \\ F_{db} &= 20 \log_{10} k \end{aligned} \quad (2)$$

and

$$\angle F = \begin{cases} 0 & : k > 0 \\ -180^\circ & : k < 0 \end{cases} \quad (3)$$

4.2 Pure derivative and factors (Pole and Zero at the origin)

$$F(j\omega) = (j\omega)^{\pm n} \quad (4)$$

The magnitude

$$F_{db} = \pm n 20 \log_{10} \omega \quad \text{for } \omega > 0 \quad (5)$$

and

$$\angle F = \pm n \times 90$$

Through the assumption of $\log_{10}\omega$ as the x -axis and the F_{dB} function as the y -axis, relation (5) shows a straight line with a slope characteristic of $\pm n 20 \text{ dB/decade}$, owing to the fact that a unity change of $\log_{10}\omega$ reflects a change of 10 in ω , i.e., a change from 2 to 20 or else 10 to 100. Small amplitude plots representative of the $n = 1, 2, -1, -2$ are reflected on the upper section of Fig. 2. The amplitude plots reflect the 0 dB line at $\omega = 1$. The phase plots are shown in the lower section of Fig. 2.

The slopes are expressed in terms of octaves. The two frequencies (which are ω_1 and ω_2) are isolated by one octave if $\omega_2 / \omega_1 = 2$. Besides, they are separated by a decade if $\omega_2 / \omega_1 = 10$. So in $\log_{10}\omega$ scale, the number of decades between any two arbitrary frequencies ω_3 and ω_4 is obtained as

$$N_{decades} = \frac{\log_{10} \frac{\omega_2}{\omega_1}}{\log_{10} 10} = \log_{10} \frac{\omega_2}{\omega_1}, \text{ Whereas the number of octaves between them, is found as}$$

$N_{octaves} = \frac{\log_{10} \frac{\omega_2}{\omega_1}}{\log_{10} 2} = 3.01 \log_{10} \frac{\omega_2}{\omega_1} = 3.01 N_{decades}$, (Using the above relation). So the slope of $\pm n$ 20 dB/decades is equivalent to $\pm n$ 6 dB/octave.

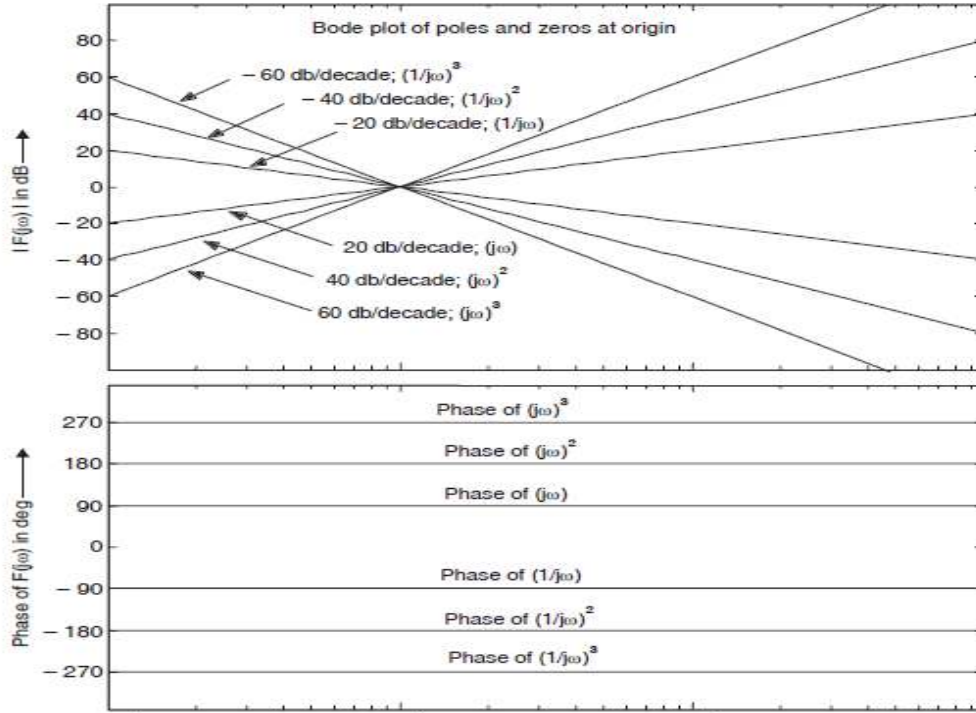


Fig. 2. Amplitude and phase plots of poles and zeros at the origin [22]

4.3 Factors characteristic to simple poles and zeros: $F(j\omega) = (1 + j\omega T)^{\pm 1}$

The log magnitude as a property of the first-order factor is expressed by the Amplitude

$$F_{ab} = \pm 20 \log_{10} \sqrt{1 + (\omega T)^2} \tag{6}$$

$$= \begin{cases} \pm 20 \log_{10} \omega T, & \omega T \gg 1 \\ 0, & \omega T \ll 1 \end{cases} \tag{7}$$

The amplitude plot can be estimated by two straight lines,

- (i) One with a slope of ± 20 dB/decade or ± 6 dB/octave and passing through frequency $\omega = 1/T$, known as corner frequency,
- (ii) The other factor is coincidental to the 0 dB line. The actual plot strategy asymptotically to the straight lines and are characterized by a maximum error of ± 3 dB happening at the corner frequency. It can be noted that the positive sign and the subsequent relations are associated with the positive power of the factor; however, the negative sign was interpreted as the negative power of the factor.

The phase angle of the first-order factor is given by:

$$\angle F(j\omega) = \pm \tan^{-1}(\omega T) = \begin{cases} 90^\circ, & \text{for } \omega T \gg 10 \\ 0^\circ, & \text{for } \omega T \ll 0.1 \end{cases} \quad (8)$$

The phase angle may also be approximated from $\frac{0.1}{T} < \omega < \frac{10}{T}$, by a straight line joining the points $(\frac{0.1}{T}, 0^\circ)$ and $(\frac{10}{T}, \pm 90^\circ)$ that passes through 45° at $\omega = 1/T$. The maximum error between the exact plot and the straight line approximation is found to be within 5.5° . Fig. 3 and Fig. 4 show typical plots for $n = 1$ and $n = -1$ respectively.

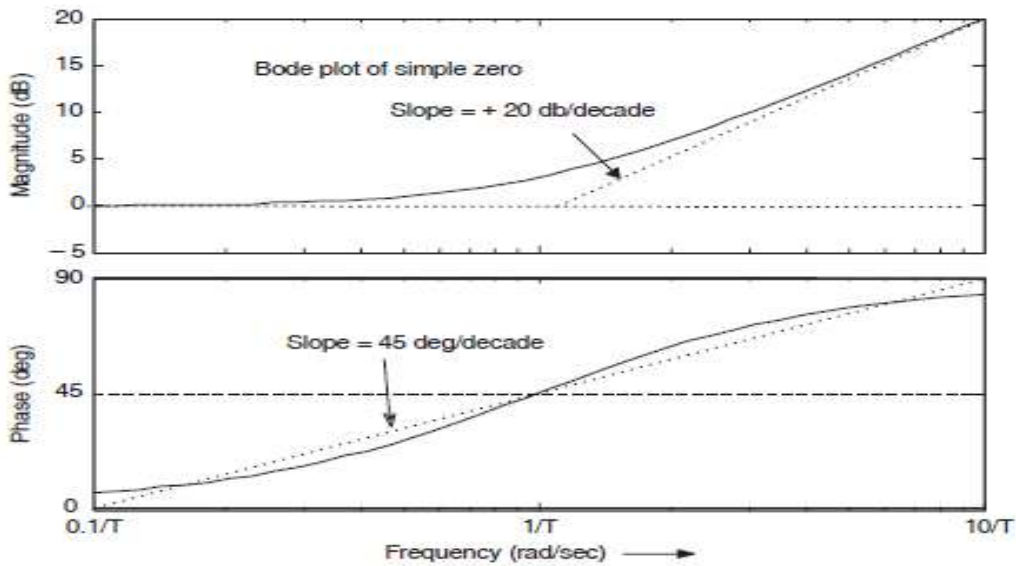


Fig. 3. Bode plot of simple zero, $F(j\omega) = (1+j\omega T)$ [22]

Bode plots are widely employed in the initial stages of the analysis and the design of the control system since it provides the nature of the frequency-response features are accurate with a minimum amount of the calculation. After the design process is complete, the simulation of the overall system was carried out for the final implementation.

4.4 Characteristic Factors of the complex poles or zeros: $[1 + 2\delta + (j\omega/\omega_n)^2]^{\pm 1}$.

The quadratic elements of the form below are encountered in the control systems:

$$F(j\omega) = \frac{1}{1 + 2\delta \left(\frac{j\omega}{\omega_n}\right) + \left(\frac{j\omega}{\omega_n}\right)^2} \quad (9)$$

The properties of the roots in the above function depend on the values of δ . For $\delta > 1$. The roots would be real as well as the quadratic factor being expressed as the product of the two first-order factors with actual poles. The quadratic factors could be expressed as the product of the two complex conjugate determinants

for the values of δ satisfying $0 < \delta < 1$. The asymptotic expressions of the frequency response curves would not be precise for the quadratic factors for the small values of δ . It is because the magnitude and the phase of the quadratic factors are determined by both the damping ratio δ and the corner frequency. The asymptotic frequency-response function was given by

$$F_{dB} = 20 \log_{10} \left| \frac{1}{1 + 2\delta \left(j \frac{\omega}{\omega_n}\right) + \left(j \frac{\omega}{\omega_n}\right)^2} \right| \quad (10)$$

$$= -40 \log_{10} \left(\frac{\omega}{\omega_n} \right), \text{ for } \omega \gg \omega_n$$

$$= 0 \text{ for } \omega \ll \omega_n$$

The frequency ω_n represents the corner frequency of the considered quadratic factor. The high frequency and low frequency asymptotes are associated with the independent of the value of δ . The resonant peak is observable near the frequency $\omega = \omega_n$ that is also depicted by Equation (10). The magnitudes of the resonant peaks are influenced by the damping ratio δ . The straight line estimation of the frequency response by asymptotes would be erroneous. The size of the error is determined by the value of δ . A large magnitude is achieved with the small value of δ .

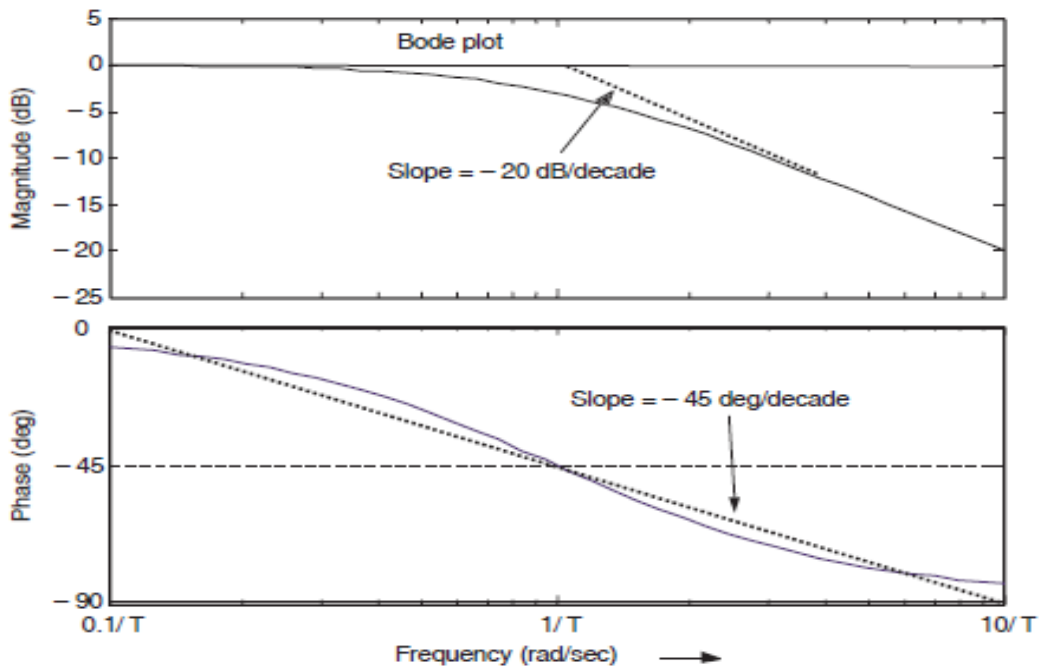


Fig. 4. Bode plot of simple pole, $F(j\omega) = (1 + j\omega T)^{-1}$ [22]

The phase angle of the quadratic factor $\left[1 + 2\delta \left(j \frac{\omega}{\omega_n}\right) + \left(j \frac{\omega}{\omega_n}\right)^2\right]^{-1}$ is given by

$$\angle F(j\omega) = -\tan^{-1} \left[\frac{2\delta \frac{\omega}{\omega_n}}{1 - \frac{\omega^2}{\omega_n^2}} \right] \quad (11)$$

The phase angle was observed to depend on δ and ω . It was 0° at $\omega=0$ and -90° with a corner frequency $\omega = \omega_n$; whereas, the phase angle approaches -180° as $\omega \rightarrow \infty$. Besides, the phase angle at the corner frequency was not determined by δ , since

$$\angle F(j\omega) = -\tan^{-1}\left(\frac{2\delta}{0}\right) = -\tan^{-1}\infty = -90^\circ \quad (12)$$

Even though asymptotic lines cannot be utilized for the amplitude and the phase plots for quadratic factors. A template that is prepared with the typical features of δ might be kept ready as to support the generation of a rough sketch. Through the application of MATLAB control Toolbox, the Bode plot of the frequencies w_{\min} and w_{\max} of the transfer function F, was expressed in accordance with its poles and zeros, can be determined by the command Bode [F,(w_{\min} , w_{\max})].

Stability could be checked in a closed-loop Bode plot and system could be designed for robustness [23]. The gear ratio gain, G_r , is the ratio of the magnitude of steady-state step response to the magnitude of the step input.

5 Results and Discussion

Results showed that when the gear ratio is less than 3, the output voltage of the system is less than the input voltage. When the gear ratio is equal 3, the output voltage is equal to the input voltage and when the gear ratio more than 3, the output voltage is greater than the input voltage.

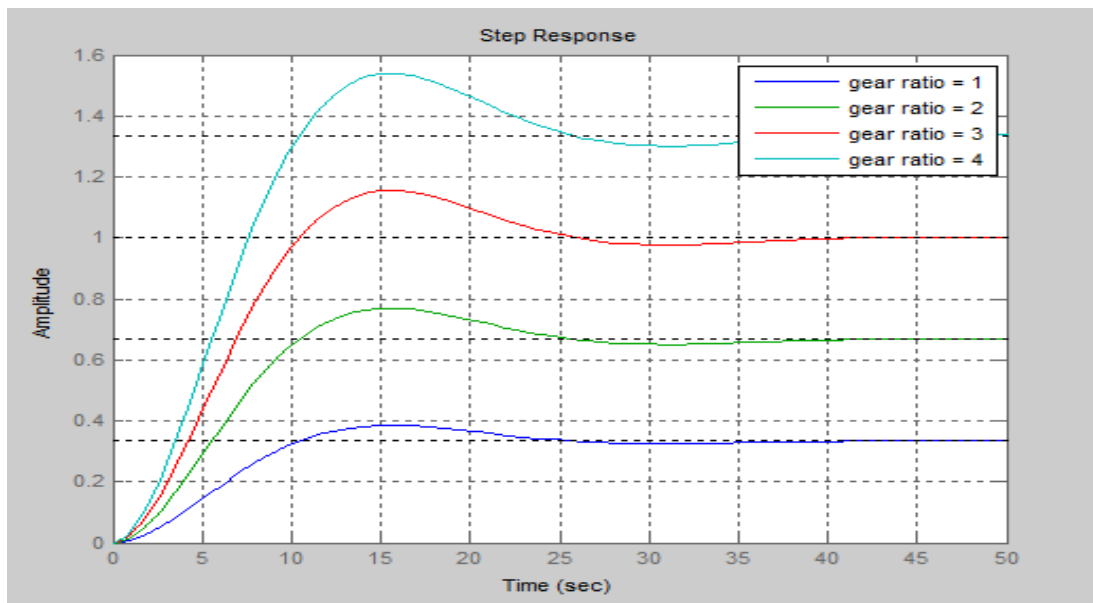


Fig. 5. Step response of the system for different values of gear ratio

The Bode response plot was necessary to examine the stability of the loop. Gear ratio G_r is a proportional value that shows the relationship between the magnitudes of the input to the magnitude of the output signal at the steady state. Many systems harbor a method by which the gear ratio can be altered, providing more or less power to the system. However, increasing gear ratio or decreasing gear ratio beyond a particular safety zone can cause the system to become unstable. As the gear ratio to the system increases, generally the rise-time decreases, the percent overshoot increases, and the settling time increases. Bode plots were determined graphically using MATLAB software.

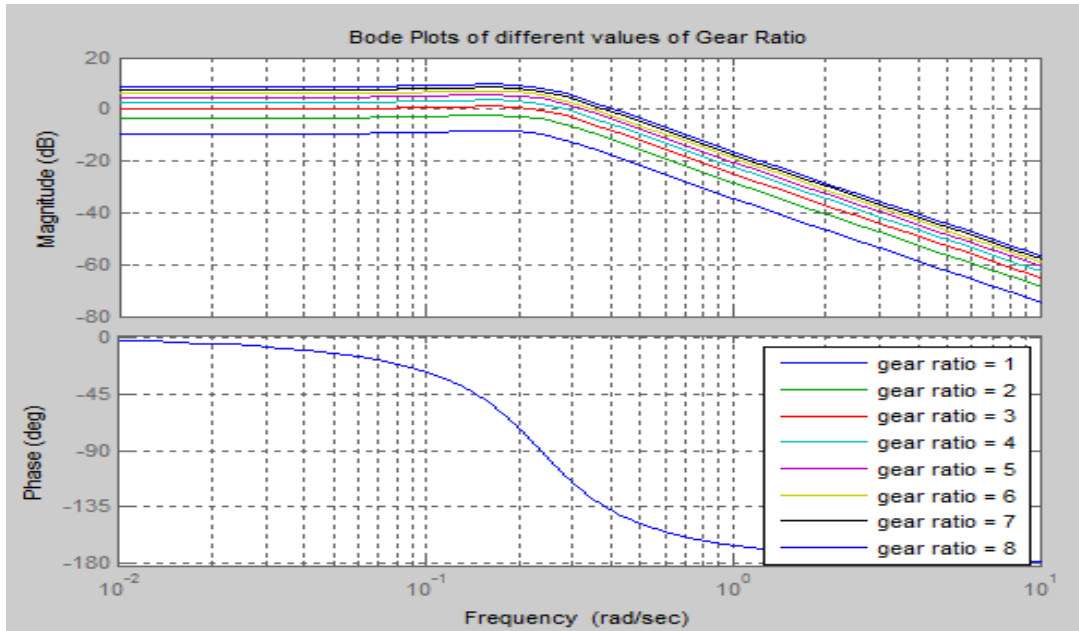


Fig. 6. Bode plot for specified values of gear ratio

The simulation results indicated that

$G_r = 1$, the system is stable and with slow response.

$G_r = 3$, the system is stable and with good step response.

$G_r = 8$, the system is unstable and with no response. The description is summarized in the table below.

Table 1. Phase margin and gain margin of the different values of the gear ratio

Gear ratio	Phase margin (deg)	Gain margin (dB)	Steady state	Overshoot (%)	Peak value	Settling time (S)	Rise time (S)
1	Inf.	Inf.	0.385	15.5% at 15.8 s	0.385	33.7	7.08
2	Inf.	Inf.	0.769	15.5% at 15.8 s	0.769	33.7	7.08
3	92.5	Inf.	1.000	15.5% at 15.8 s	1.150	33.7	7.08
4	68.8	Inf.	1.330	15.5% at 15.8 s	1.540	33.7	7.08
5	57.5	Inf.	1.670	15.5% at 15.8 s	1.920	33.7	7.08
6	50.4	Inf.	2.000	15.5% at 15.8 s	2.31	33.7	7.08
7	45.3	Inf.	2.330	15.5% at 15.8 s	2.69	33.7	7.08
8	41.5	Inf.	2.670	15.5% at 15.8 s	3.08	33.7	7.08

6 Conclusion

From Table 1, it was observed that the gain margin is increasing with an increase in the gear ratio. Using stability criterion [21], in order to have a nice power supply the phase margin should be greater than 45° and the gain margin should be greater than 10dB. Therefore, the power supply is very good for the range $1 \leq G_r \leq 7$. This indicates a phase margin of above 45° and the corresponding closed-loop step response exhibits 15.5 % overshoot and some oscillations.

Acknowledgement

I am grateful to the funding received from National Research Funds (NRF NATIONAL CALL PROPOSAL 2016/2017 PHD/159), Furthermore, this research has attracted grants from Moi University through partial scholarship and research fund for postgraduate research and training, 2016.

Competing Interests

Author has declared that no competing interests exist.

References

- [1] Venkata S, Eremia M, Toma L. Background of power system stability. Handbook of Electrical Power System Dynamics: Modeling, Stability, and Control. 2013;453-475.
- [2] Aström KJ, Murray RM. Feedback systems: An introduction for scientists and engineers. Princeton University Press; 2010.
- [3] Kumar P. Control: A perspective. Automatica. 2014;50(1):3-43.
- [4] Tashakori S, Tavakoli A, Mirzaei F. Effective micro grid stability under excitation limiters in islanded and connected modes. American Journal of Electrical and Electronic Engineering. 2017;5(1):28-33.
- [5] Hashemian R. S-plane bode plots-identifying poles and zeros in a circuit transfer function. In Circuits & Systems (LASCAS), 2015 IEEE 6th Latin American Symposium on. 2015. IEEE.
- [6] Radovanović M, Potrebić M, Tošić DV. Extraction of zeros and poles of combline filters. in Telecommunications Forum (TELFOR), 2012 20th. 2012. IEEE.
- [7] Akgül A. Obtaining real-time Bode (analysis) of electronic circuits with LabVIEW. Fen Bilimleri Enstitüsü dERGİSİ. 2017;706.
- [8] Blanchard ED, Smith MJ, Nguyen CH. Parameter identification study of frequency response data for a trilayer conjugated polymer actuator displacement model. In Advanced Intelligent Mechatronics (AIM), 2013 IEEE/ASME International Conference on. 2013. IEEE.
- [9] Gardner MJ, Barnes L. Transients in linear systems. Wiley New York. 1942;1.
- [10] Berdahl EJ. Applications of feedback control to musical instrument design. Stanford University; 2010.
- [11] Gardner FM. Phaselock techniques. John Wiley & Sons; 2005.
- [12] Davis D, Patronis E. Sound system engineering. CRC Press; 2014.
- [13] Ayllon N, et al. Systematic approach to the stabilization of multitransistor circuits. IEEE Transactions on Microwave Theory and Techniques. 2011;59(8):2073-2082.
- [14] Jian-Shu L, Yu-Shu C, Leung AY. Robust control of periodic bifurcation solutions. Applied Mathematics and Mechanics. 2004;25(3):263-271.

- [15] Juan C, Weisha H, Qing G. A new design method of internal model control based on butterworth filter for non-minimum phase high-order systems. in Control Conference (CCC), 2015 34th Chinese. IEEE; 2015.
- [16] Walsh GC, Ye H, Bushnell LG. Stability analysis of networked control systems. IEEE Transactions on Control Systems Technology. 2002;10(3):438-446.
- [17] Antonelli G. Stability analysis for prioritized closed-loop inverse kinematic algorithms for redundant robotic systems. IEEE Transactions on Robotics. 2009;25(5):985-994.
- [18] Orazem ME, Tribollet B. Electrochemical impedance spectroscopy. John Wiley & Sons. 2011;48.
- [19] Koech W, et al. Dynamic model of a DC Motor-Gear-Alternator (MGA) system. Asian Research Journal of Mathematics; 2016.
- [20] Koech W, et al. Parameter estimation of a DC Motor-Gear-Alternator (MGA) system via step response methodology. American Journal of Applied Mathematics; 2016.
- [21] Shirsavar A. Designing stable digital power supplies. Biricha Digital Power Ltd. 2011;3.
- [22] Mandal AK. Introduction to control engineering: Modeling, analysis and design. New Age International; 2006.
- [23] Chen MC. Robust estimation with dynamic integral quadratic constraints; 2013.

© 2017 Koech; This is an Open Access article distributed under the terms of the Creative Commons Attribution License (<http://creativecommons.org/licenses/by/4.0>), which permits unrestricted use, distribution, and reproduction in any medium, provided the original work is properly cited.

Peer-review history:

The peer review history for this paper can be accessed here (Please copy paste the total link in your browser address bar)

<http://sciencedomain.org/review-history/21746>